MLM--3258

DE85 014402

Mound Activities in Chemical and Physical Research: July-December 1984

Issued: June 17, 1985

MOUND FACILITY
Miamisburg, Ohio 45342

operated by
MONSANTO RESEARCH CORPORATION
a subsidiary of Monsanto Company

for the
U. S. DEPARTMENT OF ENERGY

Contract No. DE-AC04-76-DP00053

Foreword

This report is issued semiannually by Mound. Under the sponsorship of the DOE Division of Basic Energy Sciences, Mound is responsible for research in the physical sciences to further the progress of science and technology in the publish interest. This report is submitted by B. R. Kokenge, Director of Nuclear Operations, and R. E. Vallee, Manager of Technology Applications and Development, from contributions prepared by W. M. Rutherford, Science Fellow (Thermal Diffusion); W. L. Taylor, Science Fellow (Gas Dynamics and Cryogenics); G. L. Silver, Science Fellow (Separation Chemistry); C. J. Wiedenheft, Leader, Metal Hydride Research; and from members of the Isotope Separation Section: W. R. Wilkes, Isotope Separation Manager; E. D. Michaels, Leader, Isotope Separation Research and Development.

These reports are not intended to constitute publication in any sense of the word. Final results either will be submitted for publication in regular professional journals or will be published in the form of MLM topical reports.

Previous reports in this series are:

MLM-2506	MLM-2884
MLM-2555	MLM-2892
MLM-2590	MLM-2998
MLM-2654	MLM-3072
MLM-2727	MLM-3125
MLM-2756	MLM-3150
MLM-2089	MLM-3195

Contents

I. Low Temperature Research

Deuterium Triple Point Temperature Standard

G. T. McConville

New results have been obtained in the cooperative program [1] with the Institute of Metrology "G. Colonnetti" (MGC) in Turin, Italy, to develop a fixed point temperature at the triple point of D_2. Franco Pavese of the Metrology Institute has proposed introducing the D_2 fixed point in the 1986-88 revision of the International Practical Temperature Scale. We have delivered a specially prepared stainless steel cell containing 70 atm very pure D_2 (HD = 60 ppm). The cell was etched to remove Fe from the surface and then vacuum baked to remove protium from the cell. The Fe is removed from the surface because water molecules hitting the surface form ferrous hydroxide plus a proton which easily diffuses in the stainless steel. The Fe is a much better source of H^+ than Ni or Cr.

The triple point measured in this cell was compared to the other D_2 cells measured at IMGC. The IMGC cells were filled in 1978 with "chemically pure" D_2, and the triple point temperature was reported at the 5th Temperature Symposium [2]. Two other measurements were reported [3,4], and the three temperatures differed by 0.03 K where accuracies of ±0.001 were claimed. The differences were traced to different amounts of HD in the three cells [5]. Thus, we proposed constructing a cell with a minimum of HD. The triple point was remeasured in IMGC cells at the same time as in the new cell. The triple point temperature in the new cell is higher because of the purer D_2. When measured on the National Physical Laboratory IPTS-68 scale, the initial triple point temperature in the new cell is 18.734 K compared to 18.729 K measured in IMGC Cell(2) in 1978. The measurement in Cell(2) in 1984 agreed with the 1978 determination to within 0.1 mK [6]. If this value is corrected for the presence of 0.4 ± 0.1% HD, it is increased so that one has 18.734 ± 0.001 K agreement for the three cells.

The normal D_2 in the solid or liquid phase at approximately 20 K converts to equilibrium D_2. In a clean metallic container, D_2 normally converts two or three times faster than in theory. The hope was that the ultra-clean Quantum Mechanics surface would reduce the conversion rate. What actually happened is shown in Figure I-1. The rate is 10 times faster than in the IMGC cells. In the first 20 hr, it was not possible to obtain a temperature plateau. The first one shown in Figure I-1 near 25 hr shows a considerable temperature increase during the conversion from solid to liquid in the cell. As the time the cell was near 18 K increased, the conversion rate decreased, and the temperature increase on the plateau becomes much smaller. Such a plateau, if it could be made to occur in the first hour, could be used as a fixed point.

A second cell, built with 304 stainless steel with no Fe removal from the surface, was treated by soaking it in D_2O vapor. The surface OH radicals exchange much easier with the heavy water than with D_2 gas. The cell was filled with 70 atm D_2 (HD = 90 ppm) and transmitted to F. Pavese at the National Bureau of Standards in Washington. The triple point measurement will be made this winter in Turin. So far, no cell containing normal D_2 has been found satisfactory because of the conversion problem.

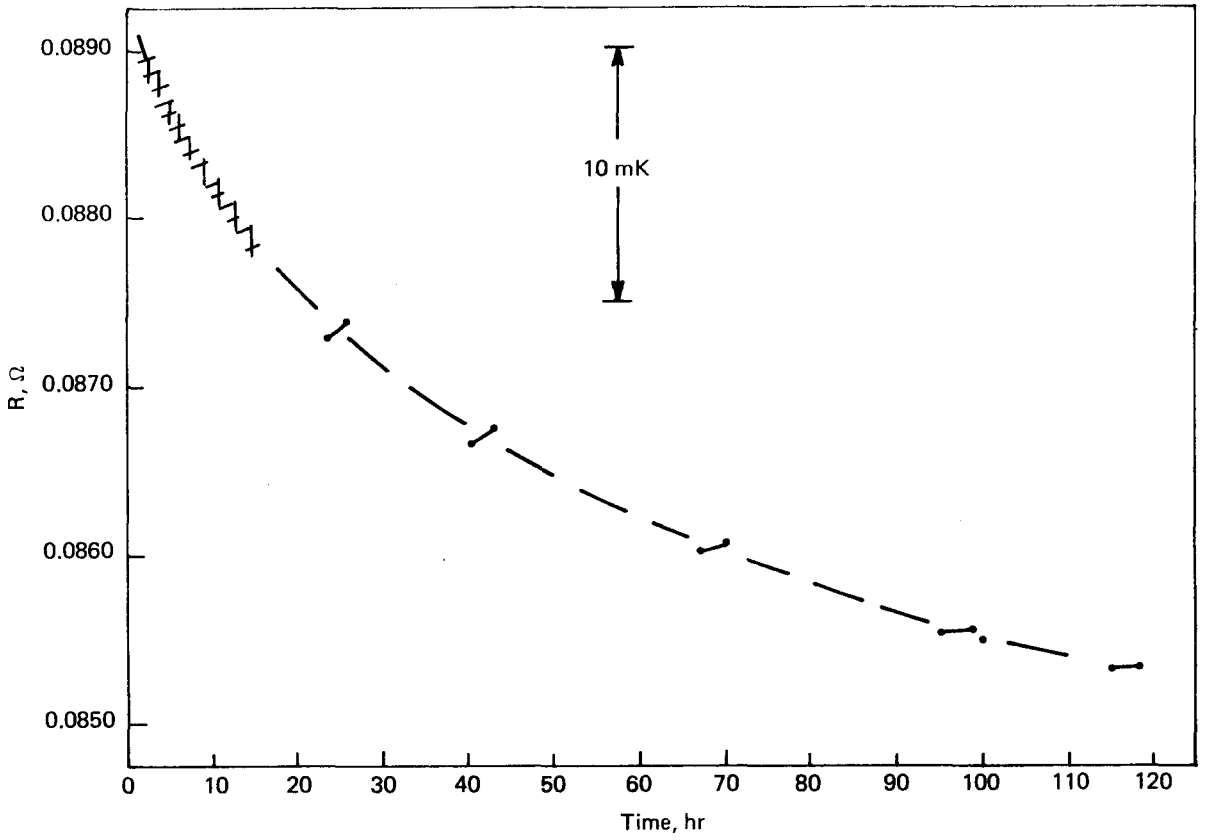

FIGURE I-1 - Time dependence of D_2 triple point temperature in Quantum Mechanics' treated cell. Symbols ⌐ represent actual triple point plateaus.

Another way to attack the conversion problem is to use a catalyst in the cell to quickly convert the normal D_2 to equilibrium D_2; i.e., to convert from a mixture in which 33% of the molecules have nuclear spins aligned parallel to a mixture in which more than 99% of the spins are anti-parallel. This fast conversion requires a highly paramagnetic third body. Normal converting catalysts such as iron or chrome alumina take about 6 hr for complete conversion. Air Products has introduced a proprietary material that converts in about 30 min. The formula for the compound is $NiSiO_4 \cdot (SiO_3)_{3.2} \cdot (H_2O)_{5.6}$. We do not know the structure of the compound. A large fraction of it is protium, which we do not want in the cell.

To replace the protium with deuterium, we first passed D_2 gas over the heated catalyst. This changed the catalyst color from light green to gray. We then learned from Air Products that heating above 125°C would destroy the catalyst structure. We next passed D_2O vapor over fresh catalyst at 120°C several times. Some of the protium was replaced. An infrared spectra trace of the processed catalyst is shown in Figure I-2. It can be seen that about 30% of the protium has been replaced by deuterium. We have obtained a Soxlet extractor which will let us keep the catalyst in the presence of the D_2O for a longer time and obtain a more complete exchange. At this time, we are able to obtain catalysts in stock from Air Products, but the company will

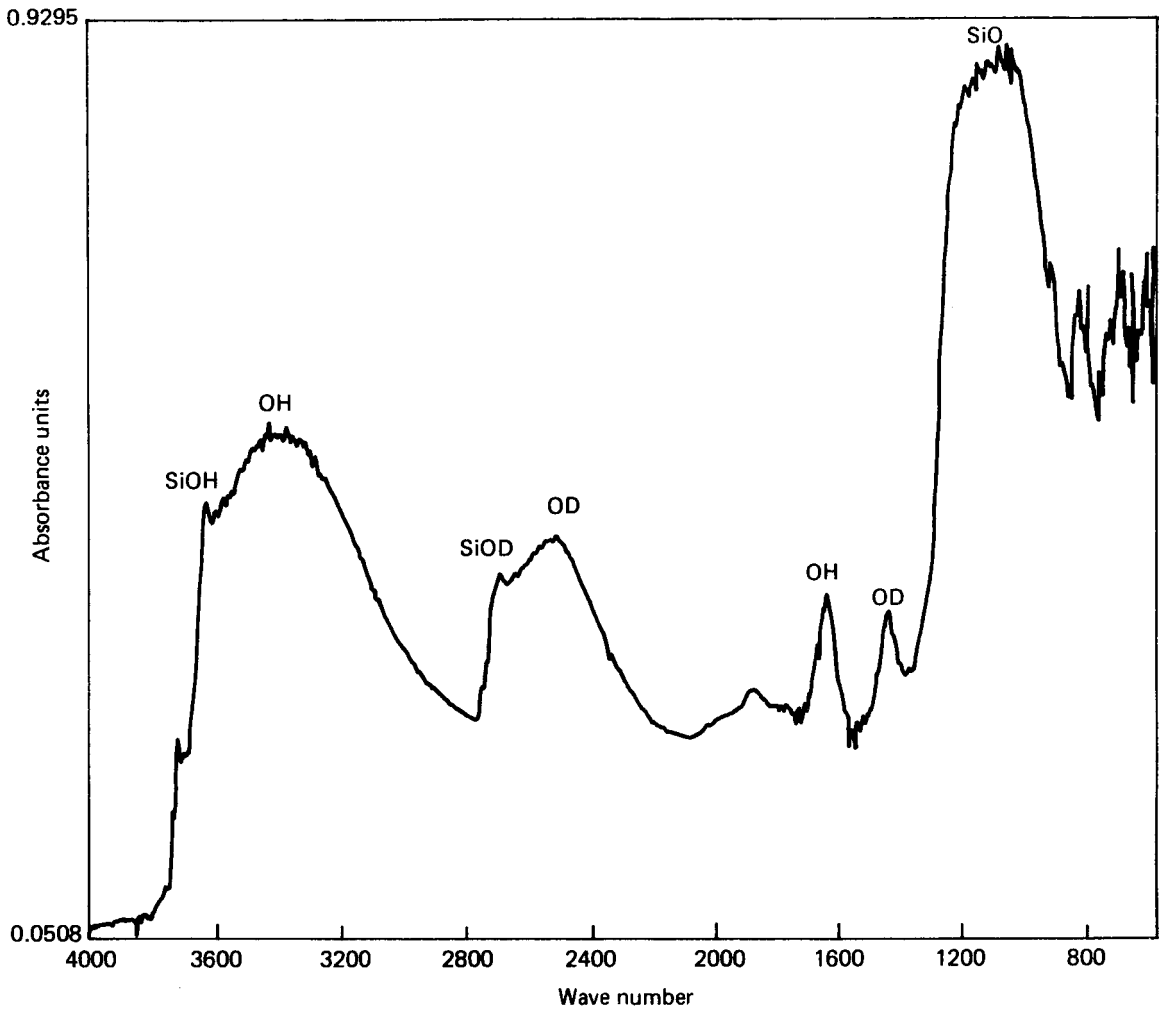

FIGURE I-2 - Infrared spectra of Air Products' catalyst showing degree of deuteration after several hours conversion at 120°C.

not attempt to make a deuterated catalyst for us. We are filling a cell with catalyst as completely exchanged as we have in order to see whether the protium left will exchange with the D_2 gas.

Helium Second Virial as Applied to Gas Thermometry

G. T. McConville

In the last progress report [7], it was shown that in order to fit the low temperature second virial data for ^4He, one must use a potential function which has a deeper minimum than the ab initio calculation of Liu and McLean [8] or the HFDHE2 function [9] which gives the best description of higher temperature data. It was also shown that a new potential form, labeled the HFIMD (Hartree-Fock + intra-atomic correlation + model dispersion) proposed by Feltgren et al. [10] could fit the low temperature data if only the inversion of their ^4He scattering data was used. Using both the ^4He data and the ^3He data produced a fit to the low temperature virial data that was higher than the upper bound on the errors in the data. Thus, the question has arisen again: Is there a real difference between ^3He and ^4He potential functions?

The two modifications to the HFDHE2 function, discussed in previous reports [7,11], were fine tuned for presentation in Karlsruhe. It was found, as shown in Figure I-3, that modifying the damping function (curve 2') or adding a $-Br^2$ term to the repulsive wall (curve A') could give essentially the same description of the ^{4}He virial as the more complicated HFIMD form. The downward arrows in the figure represent the difference from the HFDHE2 line that would give a 1 mK temperature change in a gas thermometer. The difference between the calculations and the data of Berry (■) [12] down to 3 K represents a temperature uncertainty of about 0.2 mK which is less than the operating uncertainty of the Leiden gas thermometer of 0.5 mK. The well depth, ε/k, of the functions which fit the data in Figure I-3 is between 10.90 and 10.94 K, which is deeper than the HFDHE2 at 10.80 K and the ab initio at 10.74 K. When both the ^{4}He and ^{3}He scattering data were used in determining the parameters for the HFIMD form, a well depth of 10.74 K results. Thus, if one constructed a potential form from just the ^{3}He

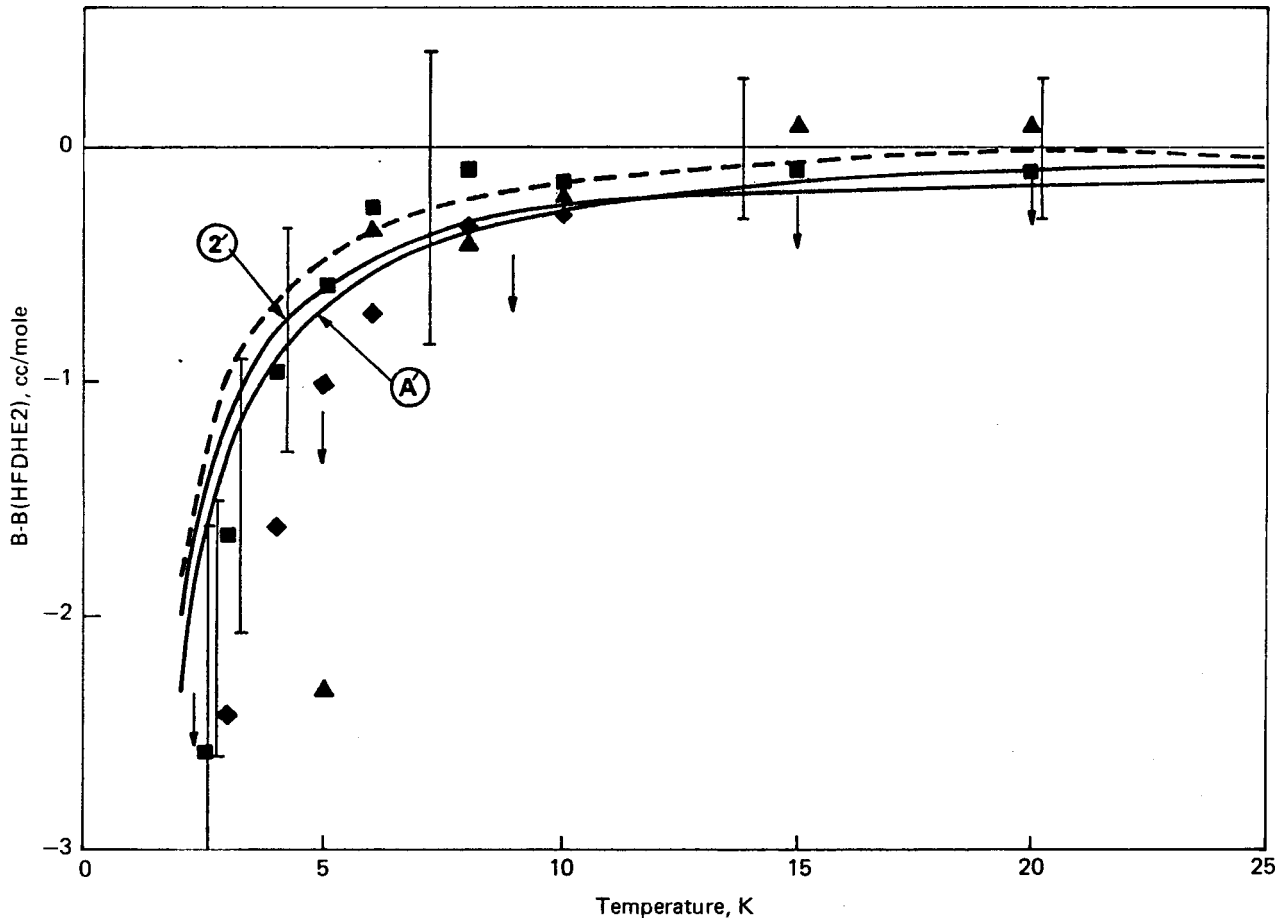

FIGURE I-3 - Calculations are compared to ^{4}He HFIMD and data: curve 2' is the form of curve 2 but with D = 1.368 giving ε/k = 10.945. Curve A' is of the form of curve A but with α = 4.48 Å^{-1}, β = 0.01 Å^{-2}, and D = 1.2585 producing ε/k = 10.90. See figures in reference 7.

scattering data, the well depth would be even smaller. This construction has not been done.

There are no ^{3}He second virial data that are of the quality of the ^{4}He data of Berry [12], Plumb [13], and Gugan [14]. There are early data of Keller [15] and Grimsrude and Werntz [16] down to 1.5 K, as well as some unpublished data of Seidel [17] down to 0.8 K. These data are compared with calculations in Figure I-4. The three calculations use the HFDHE2, the HFIMD for the ^{3}He and ^{4}He data, and the modified HFDHE with repulsive parameters $\alpha = 4.48\ \text{Å}^{-1}$ and $\beta = 0.01$ Å and $D = 1.2585$. It can be seen in Figure I-4 that the HFDHE2 and the modified HFDHE give a better representation of the ^{3}He data than the HFIMD form, which, in part, relies on ^{3}He scattering data. If the HFIMD relied only on the ^{3}He scattering data to determine the undetermined parameters [7], the curve in Figure I-4 would lie even higher above the data. This comparison indicates that Feltgren's ^{4}He scattering data [10] is more reliable than his ^{3}He scattering data. With respect to the uncertainty in the ^{3}He second virial, it is not clear in Figure I-4 whether the HFDHE2 or the modified HFDHE better represents the data. The uncertainty in Berry's ^{4}He data, shown for comparison, is an order of magnitude smaller than the ^{3}He uncertainties. It is the aim of the ^{3}He virial experiments to be done in the Kamerlingh Onnes Laboratory in Leiden to reduce the uncertainty in the ^{3}He virials to the order of Berry's uncertainty.

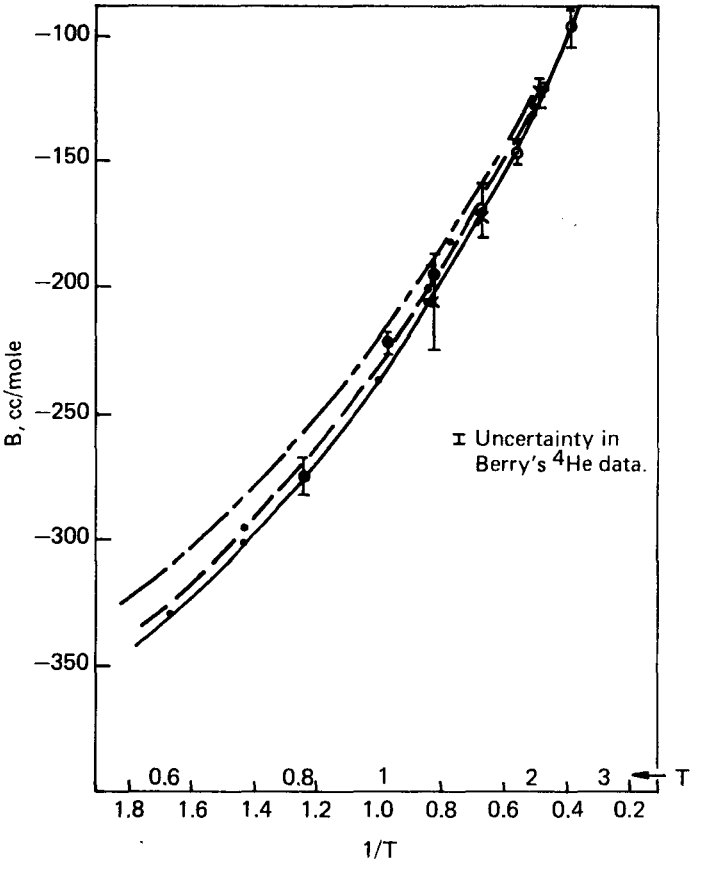

FIGURE I-4 - Comparison of calculated ^{3}He second virial to data: ⊙Keller, x Grimsrude and Werntz, ● Seidel. Calculations: --- HFDHE2, —·—HFIMD, and ___ modified HFDHE.

II. Separation Research

Liquid Phase Thermal Diffusion

W. M. Rutherford

Isotopic thermal diffusion data have been accumulated for a number of liquid compounds. Work is now in progress to correlate the thermal diffusion factor with molecular mass and structure. A previous report [1] and a forthcoming publication [2] present the results of the first attempt at such a correlation, wherein the isotopic thermal diffusion factor was related to differences in molecular masses and moments of inertia. The correlation was based on data for a series of halogen, deuterium, and ^{13}C substituted benzenes. In general, the data were represented within experimental accuracy by:

$$\alpha_T = 1.973(m_1-m_2)/(m_1+m_2) + 0.973(I_1-I_2)/(I_1+I_2), \quad (1)$$

where α_T is the thermal diffusion factor, m_1 and m_2 are the molecular masses, and I_1 and I_2 are the second moments. The data of Ma and Beyerlein [3] for two systems involving dideuterobenzenes, however, are not consistent with the above relationship.

Additional data have been acquired for deuterated benzenes and for ^{34}S substituted carbon disulfide. The new data were acquired using yet another experimental column, the design of which closely resembles that of the prototype columns used for practical scale isotope separation experiments.

The design of the new experimental column, the dimensions of which are given in Table II-1, was chosen to avoid some of the problems encountered with previous configurations. It was found, for instance, that although nickel-200 was highly desirable from the standpoint of thermal distribution, it was relatively unsatisfactory with respect to chemical resistance with the working fluid. The new column, therefore, was made from austenitic stainless steel. The massive 40-mm cold wall thickness used for previous columns did not seem to result in improved performance; thus, the wall thickness of the new column was reduced to 3 mm to obtain a more favorable temperature distribution.

Table II-1 - LIQUID PHASE THERMAL DIFFUSION COLUMN DIMENSIONS AND OPERATING CONDITIONS

Column length, mm:	457.2
Diameter of annulus, mm:	19.7
Steam temperatures, °C:	115, 164
Water temperature, °C:	15
Spacing, μm @115°C:	256
@164°C:	250

Several experiments were completed with carbon disulfide. In two of these, the separation of the $C^{32}S^{34}S/C^{32}S^{32}S$ pair was measured at steam temperatures of 164 and 115°C using carbon disulfide of natural isotopic abundance as starting material. Carbon disulfide enriched in ^{34}S was used for a third experiment at 115°C to measure, in addition, the separation of the $C^{34}S^{34}S/C^{32}S^{32}S$ pair.

Separation factors were measured as a function of time during start-up from an initially uniform composition. Experimental column coefficients H and K were derived from the data by fitting the calculated behavior of the column to the measured separations. The parameters H and K, which are defined as the initial

transport coefficient and the remixing coefficient, respectively, appear in the equation describing the transient behavior of the column:

$$\frac{\partial w_1}{\partial t} = -\frac{1}{\mu}\frac{\partial \tau_1}{\partial z} \qquad (2)$$

where w_1 is the mass fraction of component 1, τ_1 is the net vertical transport of component 1, t is time, μ is the mass held up per unit of column length, and z is the vertical coordinate. Numerical solutions of Equation (2) were obtained through the use of computer program MTRAN [4,5], and the values of H and K were adjusted to give the best least squares match to the separation data.

Results from the carbon disulfide measurements are given in Table II-2 along with pertinent column operating parameters. The thermal diffusion factors which appear in Table II-2 were calculated from the initial transport coefficient by:

$$\alpha_T = H/\xi \qquad (3)$$

Table II-2 - LIQUID PHASE THERMAL DIFFUSION EXPERIMENTS WITH CARBON DISULFIDE

Experiment 1, Natural Feed at a Steam Temperature of 164°C	
Hot wall temperature, °C:	148.6
Cold wall temperature, °C:	34.4
10^3K, g cm/s (exptl):	8.9
10^3K, g cm/s (theory):	8.2
10^5H, g/s:	17.7
α_T, $C^{32}S^{34}S/C^{32}S^{32}S$:	0.052
Experiment 2, Natural Feed at a Steam Temperature of 115°C	
Hot wall temperature, °C:	103.7
Cold wall temperature, °C:	28.4
10^3K, g cm/s (exptl):	3.9
10^3K, g cm/s (theory):	3.7
10^5H, g/s: $C^{32}S^{34}S/C^{32}S^{32}S$:	7.6
α_T, $C^{32}S^{34}S/C^{32}S^{32}S$:	0.051
Experiment 3, Enriched Feed at a Steam Temperature of 115°C	
Hot wall temperature, °C:	103.7
Cold wall temperature, °C:	28.4
10^3K, g cm/s (exptl):	4.2
10^3K, g cm/s (theory):	3.7
10^5H, g/s, $C^{32}S^{34}S/C^{32}S^{32}S$:	8.1
10^5H, g/s, $C^{34}S^{34}S/C^{32}S^{32}S$:	16.4
α_T, $C^{32}S^{34}S/C^{32}S^{32}S$:	0.055
α_T, $C^{34}S^{34}S/C^{32}S^{32}S$:	0.110

The quantity ξ, which is calculated from theory, is a complicated function of the properties of the fluid and the dimensions and operating conditions of the column [6].

Experimental and theoretical values of K are also given in Table II-1. A comparison of these values constitutes a sensitive test of the performance of the experimental column with respect to theory.

The two thermal diffusion factors derived from the run with enriched feed are plotted in Figure II-1 against values calculated from Equation (1). Figure II-1, which is a reproduction of the figure presented in the previous report, contains the experimental data used to develop Equation (1). The agreement between calculated and experimental values is good, considering that the equation was developed strictly on the basis of data for substituted benzenes.

The data of Ma and Beyerlein for systems involving 1,2 and 1,4 dideuterobenzene versus C_6H_6 do not agree with the predictions of Equation (1). Samples of the two isotopically substituted compounds have been purchased, and we are in the process of repeating these measurements. Preliminary results are available for the 1,2 dideuterobenzene system and for the C_6D_6/C_6H_6 system, which was run as a check.

The results of the experiments, which were done by the same techniques as those used for the carbon disulfide systems, are given in Table II-3. The thermal diffusion factor for the fully deuterated system is in good agreement with previous measurements, including the one of Ma and

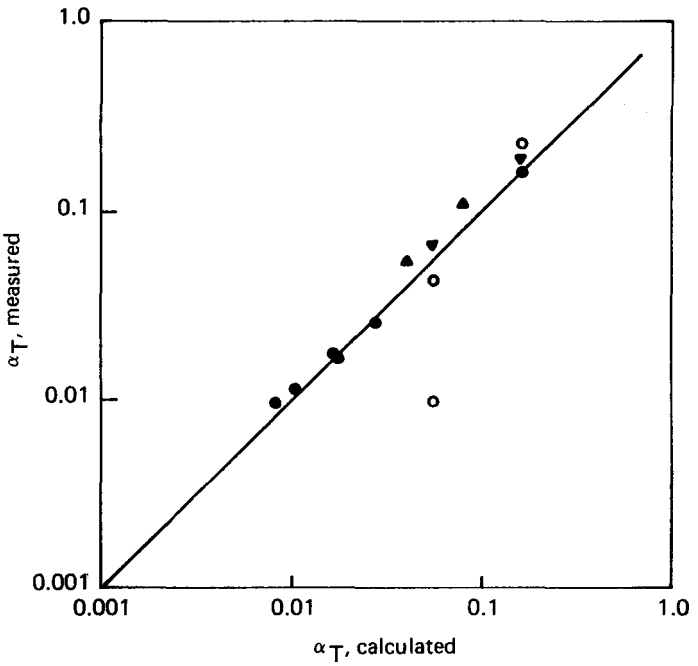

Figure II-1 - Measured versus calculated thermal diffusion factors for substituted benzenes and for carbon disulfide. The triangles, ▲, are the carbon disulfide data from this investigation and the inverted triangles, ▼, are the benzene data. The open circles, o, are the data of Ma and Beyerlein.

Beyerlein. The result for the 1,2 dideuterobenzene system, however, is more than 6 times that of Ma and Beyerlein, and it is in reasonably good agreement with the value predicted from Equation (1).

Additional work with the deuterated benzene compounds is planned, including spectroscopic measurements to verify the structure of the dideuterobenzene samples.

Calcium Isotope Separation

W. M. Rutherford

Work continued on the development of the solvent counterflow process for the separation of calcium isotopes by liquid phase thermal diffusion. We had found in experiments reported previously [7] that nickel-200 was not a satisfactory

Table II-3 - LIQUID PHASE THERMAL DIFFUSION EXPERIMENTS WITH DEUTERATED BENZENES

Experiment 1, the C_6D_6/C_6H_6 System	
Hot wall temperature, °C:	104.6
Cold wall temperature, °C:	36.4
10^3K, g cm/s (exptl):	1.04
10^3K, g cm/s (theory):	0.95
10^5H, g/s:	8.74
α_T:	0.189
Experiment 2, the 1,2 $C_6D_2H_4/C_6H_6$ System	
Hot wall temperature, °C:	103.9
Cold wall temperature, °C:	31.7
10^3K, g cm/s (exptl):	1.33
10^3K, g cm/s (theory):	1.02
10^5H, g/s:	8.74
α_T:	0.066

material of construction for the thermal diffusion columns. Prolonged exposure to concentrated aqueous calcium nitrate solutions at elevated temperatures resulted in increased pH and the concomittant deposition of insoluble calcium and nickel salts in the column annulus. Deposition of the solids led to poor and erratic performance of the apparatus with the result that we were unable to get a clear-cut evaluation of the potential usefulness of the thermal diffusion process for calcium isotope separation.

The construction and testing of a new stainless steel column have been completed. This report describes the results of those tests and their consequences in terms of cascade design and the potential practicality of the thermal diffusion process.

Stainless steel appears to be a much more satisfactory material than nickel from the standpoint of chemical resistance; however, it has a much lower thermal conductivity. The temperature distribution in a stainless steel column tends to be relatively unfavorable in that a larger fraction of the available temperature drop takes place within the column walls and a smaller fraction within the working annulus. In order to offset the lower conductivity, the new column was made of relatively thin-walled material. As tests later established, the overall result was that the effective temperature difference was reduced to approximately 85%, and the initial transport coefficient to 70% of the respective values observed for the nickel column.

The experimental apparatus and procedures were changed to provide for measurement and control of the pH of the solution at the bottom of the column. As the result of separation of the hydrogen ion, the pH at the bottom of the column tends to be higher than at the top; thus, control of the bottom at a safe value will ensure

that conditions for solid precipitation will not be reached anywhere in the system.

During each run, 50-μL samples were removed daily for pH measurement with a microelectrode. When the pH reached a value of 8.0, the solvent counterflow was switched from distilled water to 0.02 N nitric acid. Distilled water flow was resumed after the pH was reduced to 7.0. The total acid requirement for this process was on the order of 0.05 to 0.1 meq at intervals of twice a week or less.

Two separation experiments were run at calcium nitrate feed concentrations of 5 and 35 wt %, respectively. Column dimensions, operating conditions, and other pertinent data are given in Table II-4. The solvent counterflow rates given in Table II-4 were established by computer control of the bottom solute concentrations at the values listed.

The separation of the ^{40}Ca-^{48}Ca pair as a function of time during the two experiments is plotted in Figure II-2. The separation factor, q_{48}, is defined by:

$$q_{48} = (w_{48}/w_{40})_B/(w_{48}/w_{40})_T \qquad (1)$$

where w_{48} and w_{40} are the mass fractions of the two calcium isotopes in total calcium.

In order to interpret the transient separation data, it was assumed that the isotope separation process was decoupled from the solute-solvent separation. This is reasonable because the solute-solvent concentration profile is established within a few hours, and it remains invariant thereafter; whereas, the isotope separation process takes place over a period of many days.

Computer solutions of the transient problem were matched to the observed

Table II-4 - LIQUID PHASE THERMAL DIFFUSION EXPERIMENTS WITH CALCIUM NITRATE SOLUTIONS

	Experiment 1	Experiment 2
Column length, m	1.22	1.22
Nominal spacing, μm	305	305
Steam temperature, °C	164	164
Water temperature, °C	15	15
Solute concentration, top, wt %	37	4.8
Solute concentration, bottom, wt %	41	15
Counterflow rate, g/hr	0.48	1.16
$10^5 H_{SS}$, g/s	22.6	37.9
$10^5 H_{48}$, g/s	0.22	0.074
$10^3 K$, g cm/s	0.65	1.17

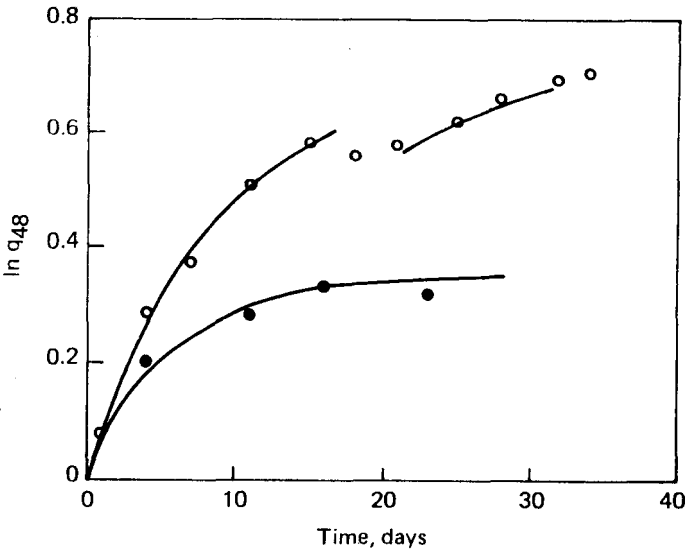

Figure II-2 - Separation of ^{48}Ca by liquid phase thermal diffusion. The upper curve and points pertain to a nominal solute concentration of 5 wt %; the lower, to 35 wt %. The solid lines are calculated. The latter part of the upper calculated curve is shifted by 7 days to accommodate the obvious discontinuity in the experiment.

separations by selecting the values of H_{48} and K which resulted in the best fit to the data. H_{48} is defined as the initial transport coefficient for the ^{48}Ca-^{40}Ca pair, and K is the isotopic remixing coefficient. These values are given in Table II-4.

Also reported in Table II-4 is H_{SS}, the initial transport coefficient for the solute-solvent pair. H_{SS} is calculated from the steady-state solvent counterflow rate by:

$$H_{SS} = \sigma/w_S \qquad (2)$$

where w_S is the mass fraction of solvent at the bottom of the column, and σ is the solvent counterflow rate.

The results of the two experiments show that the isotope separation effect is relatively large at low solute concentrations, but that it decreases significantly as the solute concentration is increased. From the practical standpoint, this is unfortunate because the isotopic transport rate is directly proportional to solute concentration; thus, to get maximum separative power, one wishes to operate a process at the highest possible concentration.

CONCEPTUAL DESIGN OF THERMAL DIFFUSION CASCADES FOR ^{48}Ca SEPARATION

The results of the two isotope separation experiments provide enough information to develop preliminary designs of thermal diffusion cascades for calcium isotope enrichment.

Two possible product specifications were considered: 1 at. % ^{48}Ca and 10 at. % ^{48}Ca. The feed material was taken to be calcium nitrate of natural isotopic abundance (0.18 at. % ^{48}Ca) and the tails composition was set at 0.16 at. %. Each cascade was composed of 3 sections. The column characteristics and solute concentration in the feed section were selected to give high isotopic transport rates; whereas, the sections toward the product end were selected for successively higher separation characteristics and correspondingly lower transport rates.

The cascade designs, the characteristics of which are given in Table II-5, were developed using the key weight method of de la Garza [8] for multicomponent systems. Column parameters of the two higher enrichment sections were taken directly from the experimental results reported above. Parameters for the feed section, which is composed of 406 μm columns, were estimated as follows:

Table II-5 - LIQUID PHASE THERMAL DIFFUSION CASCADES FOR CALCIUM ISOTOPE SEPARATION

Product composition, at. % ^{48}Ca	1	10
Feed Section		
Number of columns in series	8	10
Hot-to-cold wall spacing, μm	406	406
Solute concentration, wt %	40	40
10^5H per unit mass, g/s	0.126	0.126
Y per unit mass	0.136	0.170
Intermediate Section		
Number of columns in series	4	5
Hot-to-cold wall spacing, μm	305	305
Solute concentration, wt %	40	40
10^5H per unit mass, g/s	0.032	0.032
Y per unit mass	0.208	0.260
Product Section		
Number of columns in series	1	5
Hot-to-cold wall spacing, μm	305	305
Solute concentration, wt %	5	5
10^5H per unit mass, g/s	0.008	0.008
Y per unit mass	0.096	0.48
Flow Rates		
Product, g/day of Ca	0.097	0.0068
Product, g/year of ^{48}Ca	0.35	0.24

$$H = 1.66(a/a_r)^3 H_r \quad (3)$$

$$Y = (a_r/a)^4 Yr \quad (4)$$

where a is the hot-to-cold wall spacing, and the subscript r refers to a reference column at the same solute concentration. The quantity Y is the reduced length of the column or section as defined by

$$Y = HL/K \quad (5)$$

The cascade lengths required to reach the two specified product compositions are reasonable; however, the estimated rates of production are extremely low. The rates are clearly too low to be useful for routine separation of calcium isotopes from feed of natural isotopic abundance. The calcium isotope effect in solution thermal diffusion is moderately large but ^{48}Ca amounts to only 200 ppm of the working solution. This places an inherent upper limit on the transport rate that can be achieved using the thermal diffusion process.

Although solution thermal diffusion does not appear to be economical for processing feed of natural isotopic abundance,

it may well be useful for further enrichment of materials produced by chemical exchange.

Low Temperature Trennschaukel

W. L. Taylor

Measurement of the thermal diffusion factor, α_T, of ^4He-^{20}Ne at low temperatures has been completed, and the results of this research are summarized here. The work consisted of experimentally determining α_T for this system in the temperature range of approximately 30 to 200 K and comparing the experimental results with both classical and quantum theoretical calculations using the best available helium/neon interatomic potential. The separations achieved in the apparatus were measured in real time by sensing the thermal conductivity of the binary mixture with calibrated thermistors installed in the device, as well as by the traditional method of mass spectrometer analysis of samples taken at the end of the experiments. Details concerning the apparatus and the calibration and use of the thermistors were covered in earlier reports [9-11] in this series.

A major reason for studying the helium/neon system was pointed out in previous work [12] at Mound which investigated thermal diffusion factors of binary noble gas mixtures. The status prior to the current work is shown in Figure II-3, which illustrates the extreme scatter among several earlier measurements [13-22], as well as the need for extending measurements down to the condensation point of neon. At first glance, much of the previous work appears to be quite inconsistent. Least squaring all of the data to a function of the form $\alpha_T = A+B/T^{\frac{1}{2}} + C/T$ yields the dotted curve which is biased to the high side of the

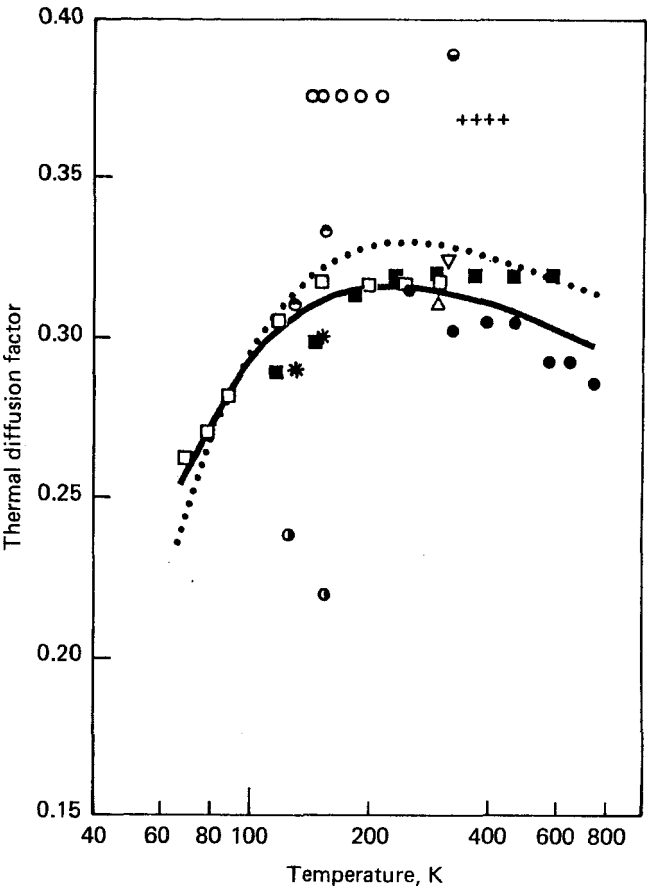

FIGURE II-3 - Previously published values of the thermal diffusion factor for an equimolar mixture of helium-neon. The experimental points are: o, Ibbs and Grew (Ref. 13); +, Puschner (Ref. 14); ⊖, Atkins, et al. (Ref. 15); ◐, van Itterbeek, et al. (Ref. 16); ■, Grew (Ref. 17); *, van Itterbeek and de Troyer (Ref. 18); ⊖, de Troyer et al. (Ref. 19); ▽, Mathur and Saxena (Ref. 20); □, Grew and Wakeham (Ref. 21); ●, Taylor (Ref. 12); and △, Trengove, et al. (Ref. 22). The dotted curve is the least square fit to all the data and the solid curve is the least square fit excluding the early data in References 13-16.

majority of points. However, if one eliminates those points which differ by more than 2 rms deviations, the solid curve is obtained with A = 0.22544; B = 2.6938; and C = -20.193. Coincidentally, the four sets of data removed [13-16] represent the four earliest

attempts to measure α_T for He-Ne. By dropping these four sets of data, the average rms percentage deviation dropped from 11.0% to 3.2%.

The new data, some of which have been discussed in previous reports [2,23] are summarized in Table II-6 and shown graphically in Figure II-4, along with the theoretical calculations. The experiments were conducted in two different pieces of equipment, and the results were analyzed by two different methods. The composition dependence was determined at an average temperature of 86 K, and several additional points were measured at 103, 130, and 203 K in a 7-tube trennschaukel described previously [24]. The compositions of the resulting samples were measured on a Consolidated Electrodynamics Corporation 620A Mass Spectrometer. The composition dependence at 86 K was found to be linear in $1/\alpha_T$ within the experimental uncertainty. The equimolar value of 0.280 was obtained from the least squares fit $1/\alpha_T = 4.717 - 2.304\ \chi_{He}$. For those points at 103, 130, and 203 K where a feed mixture other than equimolar was used, the composition dependence was calculated quantum mechanically at each temperature, and the respective measured values were adjusted to an equimolar mixture (see column 4 in Table II-6.

Table II-6 - THERMAL DIFFUSION FACTORS FOR ^4He-^{20}Ne AT LOW TEMPERATURES

Temperature (K)	Feed Composition (% ^4He)	α_T	α_T (Equimolar)	Percentage Deviation from Least Squares Fit
31	0.498	--	0.129	+1.4
31	0.498	--	0.133	+4.5
45	0.510	--	0.193	-4.0
45	0.510	--	0.191	-5.0
82	0.498	--	0.267	-1.3
82	0.498	--	0.272	+0.6
86	0.176	0.235		
86	0.351	0.264		
86	0.500	0.263	0.280	+2.1
86	0.504	0.281		
86	0.945	0.391		
86	0.947	0.410		
100	0.498	--	0.280	-1.6
100	0.498	--	0.277	-2.7
103	0.190	0.256	0.296	+3.3
125	0.501	--	0.299	+0.7
125	0.501	--	0.311	+4.7
130	0.200	0.252	0.286	-4.3
203	0.505	--	0.310	-1.3
203	0.661	0.335	0.312	-0.7

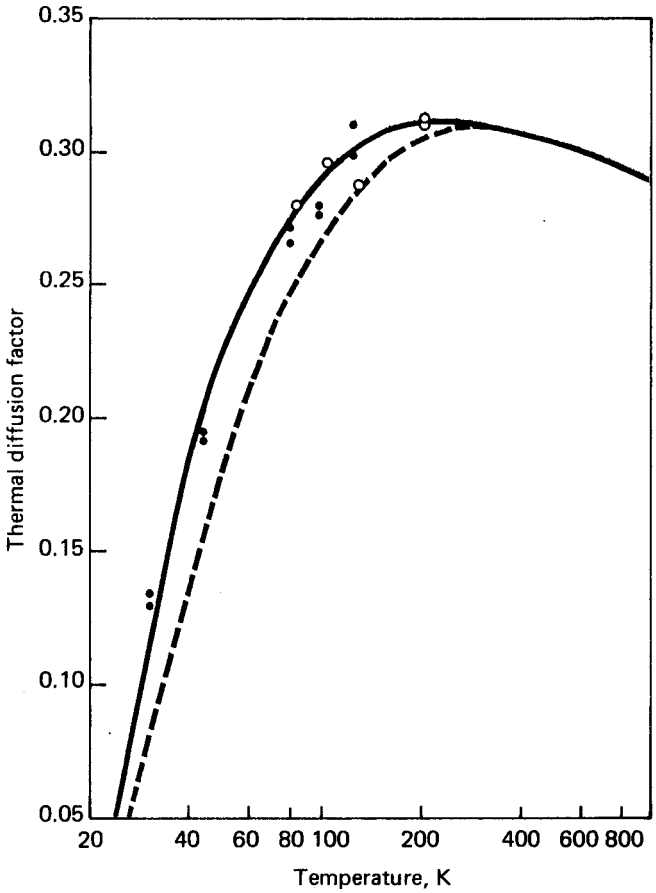

FIGURE II-4. The thermal diffusion factor of ^{4}He-^{20}Ne. The experimental points are: •, equimolar feed mixture measured in 10-tube trennschaukel; o, equimolar feed mixture measured in 7-tube trennschaukel; ⌀, feed mixture other than equimolar but corrected for composition dependence; and ⌖, equimolar value obtained from determination of composition dependence. The solid line is the quantum calculation for $[\alpha_T]_3$ described in Reference 11, and the dashed line is the equivalent calculation employing classical mechanics.

The 10-tube trennschaukel described in Reference 9 was used to measure the values at 31, 45, 82, 100, and 125 K. The additional tubes increased the separation for a given ΔT by 30%. Although the use of the in situ thermistors increased the precision of the analysis for isothermal experiments by approximately a factor of five, an experimental problem was encountered which detracted considerably from the thermistor method of analysis, especially at the lower temperatures. The problem originated in the necessity to obtain thermistor calibrations at both T_C and T_H, while the entire trennschaukel was isothermal -- a condition which was not always easily achieved. In fact, it was found impossible to hold the isothermal condition long enough at T_H in the 31 K experiments and T_C and T_H in the 45 K experiments. Compositions for those experiments were therefore analyzed with the mass spectrometer.

Thermal diffusion factors were calculated both classically and quantum mechanically using a recent and accurate potential for this system developed by Buck from the inversion of differential scattering cross sections (DSCS). This potential, with slightly modified parameters, is cited by Aziz [25] in a recent treatise on inert gases. These minor modifications were made so that the potential would predict selected transport and thermodynamic properties within their reported experimental uncertainty (as summarized by Aziz). In addition to the DSCS data, the potential reproduces Brewer's [26] second virial coefficients to within 0.14 cc/mole; the Kestin-Mason [27] viscosity correlation to within 0.56% (rms); van Heijningen's [28] diffusion data to 0.8% (rms); and the precise diffusion [29] and thermal diffusion [30] data of Dunlop to within 0.1 and 2.5%, respectively. Also, because the like-like interactions must be considered, the best available potentials for Ne-Ne [31] and He-He [32] were employed. Further details of the calculation, the specific form of the potential, and the potential parameters are given in Reference 11. The solid curve

in Figure II-4 is the quantum mechanical calculation for $[\alpha_T]_3$, the third Chapman-Cowling approximation, and the dashed curve is the classical analog. Very obviously, the quantum nature of the system is demonstrated by the clustering of the experimental points around the upper curve. The correspondence limit is around 300 K, which is reminiscent of the helium alone where the limit is only about 50 to 100 K higher. This demonstrates the strong influence of the low mass component on the de Broglie wavelength which can be anticipated by the behavior of the expression for the reduced mass of the system,

$$\frac{1}{\mu} = \frac{1}{m_{He}} + \frac{1}{m_{Ne}} .$$

The present data were least-squared to yield the equation:

$$\alpha_T = 0.32082 + 0.53662/T^{\frac{1}{2}} - 8.9893T \quad (1)$$

with an average rms percentage deviation of 3.2%. This is shown as the solid line in Figure II-5 using the quantum calculation of $[\alpha_T]_3$ as the zero or baseline. The relatively large percentage deviation at the lower temperature is actually not too surprising because the absolute value of α_T is small and decreasing rapidly in this region. The dotted curve is the percentage deviation of the least square equation given above for all previous data except that of the earliest four workers. This turns out to be amazingly close to the calculated values. The dashed line is the deviation of the classical from the quantum calculations, and this deviation is enormous in the vertical portion of the α_T curve.

In conclusion, the newly proposed 7-parameter potential, which correlates transport properties very well for a variety of systems, provides extremely

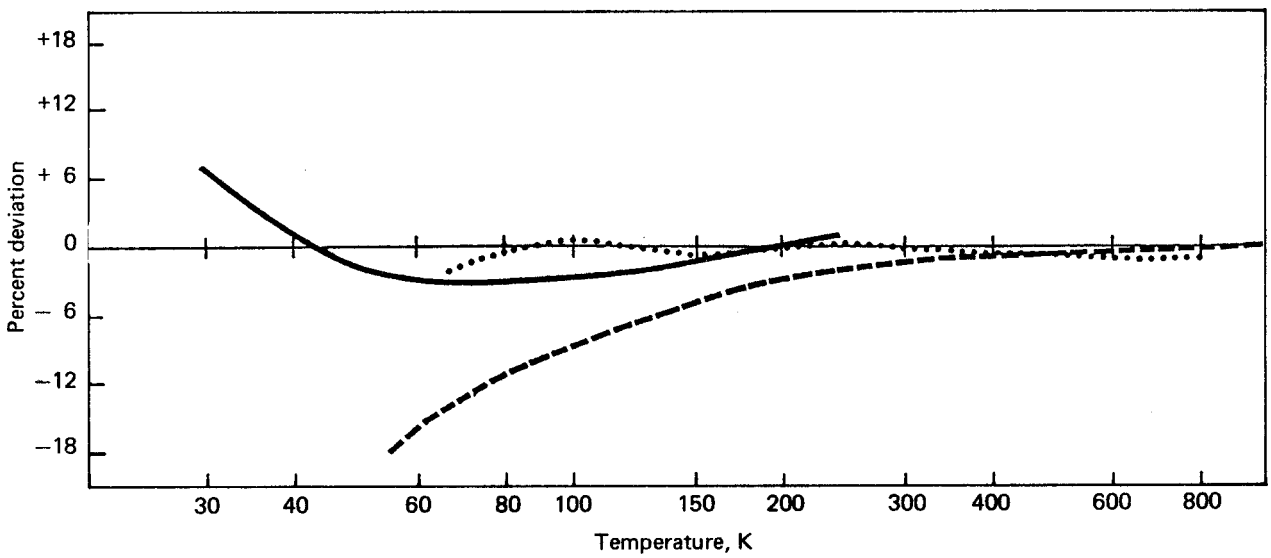

FIGURE II-5 - Percentage deviation of α_T from the theoretical value of $[\alpha_T]_3$ calculated quantum mechanically (baseline). The curves are: ——, least square expression for the present data; ...., least square expression for all previous data excluding the four earliest works; and ---, $[\alpha_T]_3$ calculated by classical mechanics.

good agreement between the quantum-mechanically evaluated α_T and the present trennschaukel data. Especially at temperatures in the 30-100 K range, the difference between quantal and classical modes of momentum transport lies heavily in favor of the quantal. From qualitative consideration of the de Broglie wavelength of the two species at these low temperatures, it becomes evident that nonclassical momentum transfer results primarily from the lower-mass component.

Calcium Isotope Effect in Calcium Ion Exchange with a Macrocyclic Compound Containing Fluid Phase

B. E. Jepson and W. F. Evans

The enrichment of calcium isotopes by ion exchange chromatography has been reported by several investigators. Generally, the single stage separation coefficients found were quite small, on the order of 10^{-4} or less, for the various systems investigated. Three exceptions are noted here. Huemann reported a separation coefficient, $\varepsilon(44/40)$, of 8.5×10^{-4} using concentrated lithium chloride as an eluent [33]. Gutsykov et al. found an $\varepsilon(44/40)$ of 41×10^{-4} using an iminodiacetate resin [34]. Our own work with calcium hydroxide ion exchange yielded an $\varepsilon(44/40)$ of 11×10^{-4} [35].

Liquid-liquid calcium chemical exchange with dicyclohexano 18-crown-6 also exhibits a large isotope effect [36], and it was of some interest to find whether this would also occur in an ion exchange system. The work below describes the results of calcium isotope exchange using ion exchange chromatography with a fluid phase containing the calcium complex of the macrocyclic compound 18-crown-6. Isotopic enrichment occurs according to the chemical exchange reaction

$$^{44}CaL^{2+} + {}^{40}Ca(SO_3R)_2 \rightleftarrows {}^{40}CaL^{2+} + {}^{44}Ca(SO_3R)_2 \quad (1)$$

where L represents 18-crown-6 and R the resin. Similar investigations have reported sodium [37] and potassium [38] isotope effects using a macrocyclic compound in conjunction with ion exchange chromatography. In the work which follows, the frontal analysis analytical technique was used to obtain the separation coefficient.

EXPERIMENTAL

Bio-Rad analytical grade sulfonic acid resin type AF-50W-X4, 200-400 mesh was used. Potassium and calcium impurities were removed by passing 4N HCl through the column until K and Ca could not be detected. This was followed by a water wash to remove excess HCl (to pH=5.5) and a final wash with a 70/30 vol % solution of ethanol/water. Potassium-free calcium was prepared according to the following steps: (1) Reagent grade $CaCO_3$ (Fischer) to $Ca(NO_3)_2$; (2) precipitation of calcium with ammonium oxalate followed by washing; (3) firing to CaO at 1000°C; and (4) preparation of an aqueous solution of $CaCl_2$. The 18-crown-6 obtained from PCR, Inc., was in the form of clear crystals and was used as received. The feed solution consisted of 70 vol % absolute ethanol and 30 vol % water with concentrations of 0.115M $CaCl_2$ and 0.121M 18-crown-6. A 6-mm i.d. column packed to a length of 94 cm with an adjustable plunger was used. The column jacket was maintained at 25.0°C. The fluid flow rate was 9.9 cc/hr and the column capacity 1442 mg of calcium.

Samples collected from the ion exchange column contained approximately 5 mg total

calcium (after the calcium breakthrough) in a matrix of 70:30 ethanol:water containing approximately 30 mg 18-crown-6. The calcium present in the samples was isolated by evaporation of the ethanol and water with controlled heating via infrared lamps and pyrolysis of the 18-crown-6 at 750 to 800°C in air. Conversion of the $CaCl_2$ to $Ca(NO_3)_2$ was effected by addition of concentrated HNO_3 (5.0 mL) and evaporation to dryness. Spot tests with $AgNO_3$ indicated complete conversion with a single addition/evaporation cycle. Following conversion to CaO at 1000°C in air, the calcium contents of the samples were determined gravimetrically. The total calcium present in the sample as obtained directly from the column was derived by applying a correction factor for any material removed. Measurement of calcium concentrations by atomic absorption for selected samples indicated <2% relative variance between atomic absorption and gravimetric methods.

Samples were diluted to a calcium concentration of 1 mg/mL with 2 N HNO_3 for isotopic analysis. Special care was exercised during all sample processing steps to prevent contamination with potassium, which interferes with calcium isotope ratio measurements. Isotopic ratios were obtained with a 15-in., 90° gas mass spectrometer modified with an LANL-designed source for solids analyses by thermal ionization. The instrumental variance over time, as estimated by repetitive analyses of a natural abundance standard, was better than ±0.05% (standard deviation) for the $^{40}Ca/^{44}Ca$ ratio. The standard deviations for the sample $^{40}Ca/^{44}Ca$ ratio measurements ranged from 0.03 to 0.37% of the ratio.

RESULTS AND DISCUSSION

The calcium breakthrough curve is shown in Figure II-6 along with the corresponding calcium 40/44 isotope ratios. The single-stage separation coefficient, ε, was calculated from the initial transport equation which can be written:

$$\tau_o = \Sigma g_i (N_i - N_o) = \varepsilon Q N_o (1 - N_o)$$

where τ_o = net transport of the isotope

g_i = mg total calcium in the ith sample

N_i = atom fraction of isotope in the ith sample

N_o = atom fraction of isotope in feed

Q = mg total calcium on resin

The results of this calculation yielded an $\varepsilon(44/40)$ of $(4.9 \pm 1.3) \times 10^{-4}$ (95% C.L.). The standard deviation was obtained from a least squares analysis. The breakthrough of 18-crown-6 first occurred at an elution volume of 20 cm³, whereas 320 cm³ were eluted before the calcium breakthrough occurred. The free fluid volume in the column was estimated to be 8 to 10 cm³, thus it is evident that some crown compound was retained on the resin. Measurements of the quantity of crown on the resin have not been completed. It is probable that a second exchange reaction occurs as follows:

$$CaL^{2+}_{fluid} + {}^{*}CaL^{2+}_{resin} \rightleftarrows {}^{*}CaL^{2+}_{fluid} + CaL^{2+}_{resin} \qquad (2)$$

This exchange occurs in parallel with the exchange reaction (1) shown above.

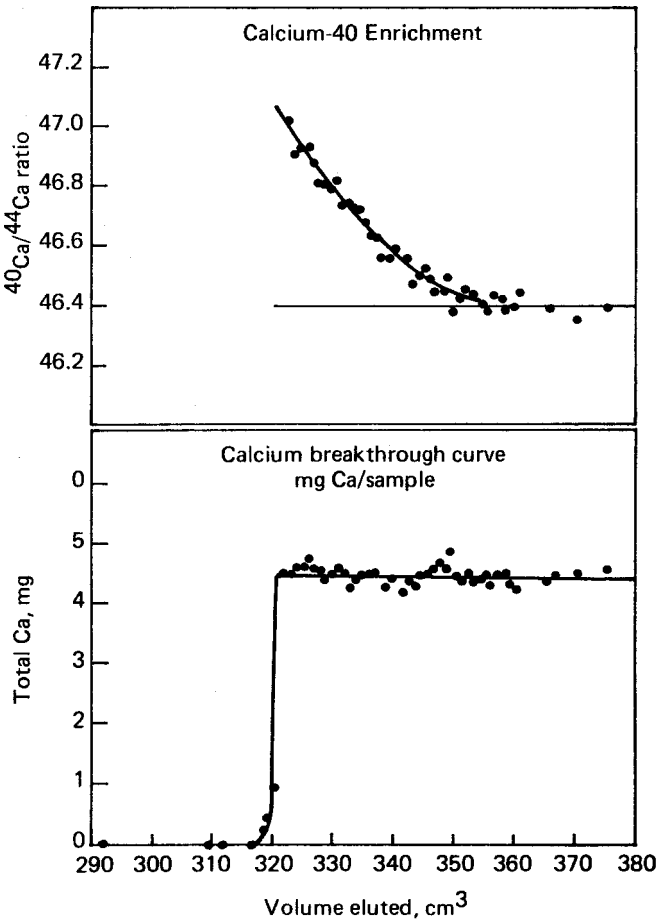

FIGURE II-6 - Calcium isotope enrichment and calicum breakthrough curve.

The separation factor ($\alpha = 1 + \varepsilon$) of 1.00049 was smaller than anticipated. Any isotope effect involving reaction (2) is expected to be small and this, in part, would explain the small size of the experimentally observed isotope effect. The stability constant of the calcium-crown complex in alcohol solutions is large and the fraction of uncomplexed calcium in the fluid was not significant.

References

I. Low Temperature Research

1. Mound Activities in Chemical and Physical Research: July-December 1982, MLM-3072, Monsanto Research Corporation, Miamisburg, Ohio (June 1983), pp. 10-11.

2. Pavese, F. Temperature, Its Measurement and Control in Science and Industry, Volume 5, 209 (1982).

3. Kemp, R. C., Temperature, Its Measurement and Control in Science and Industry, Volume 5, 249 (1982).

4. Ancsin, J., NRC Canada, private communication, 1981.

5. McConville, G. T., and D. A. Menke, Temperature, Its Measurement and Control in Science and Industry, Volume 5, 147 (1982).

6. Pavese, F., Comite' Consultatif de Thermometrie, 1984.

7. Mound Activities in Chemical and Physical Research: January-June 1984, MLM-3195, Monsanto Research Corporation, Miamisburg, Ohio (October 1984), pp. 10-14.

8. Liu, B., and A. D. McLean, J. Chem. Phys., 59, 4557 (1973).

9. Aziz, R. A., V.P.S. Nain, J. S. Carley, W. L. Taylor, and G. T. McConville, J. Chem. Phys., 70, 4330 (1979).

10. Feltgren, R., H. Kirst, K. A. Kohler, H. Pauly, and F. Torello, J. Chem. Phys., 76, 2360 (1982).

11. Mound Activities in Chemical and Physical Research: July-December 1983, MLM-3150, Monsanto Research Corporation, Miamisburg, Ohio (June 1984), pp. 10-11.

12. Berry, K. H., Temperature, Its Measurement and Control in Science and Industry, James F. Schooley, ed., APS 1983, pp. 21-24.

13. Plumb, H. H., Temperature, Its Measurement and Control in Science and Industry, James F. Schooley, ed., APS 1983, pp. 77-78.

14. Gugan, D., Metrologia, 19, 147 (1984).

15. Keller, W. E., Phys. Rev., 97, 1 (1955).

16. Grimsrude, D. T., and J. H. Werntz, Phys. Rev., 157, 181 (1967).

17. Seidel, G., Brown University, private communication, 1984.

II. Separation Research

1. Mound Activities in Chemical and Physical Research: January-June 1984, MLM-3195, Monsanto Research Corporation, Miamisburg, Ohio (October 1984), p. 17.

2. Rutherford, W. M., J. Chem. Phys., in press.

3. Ma, N. R., and A. L. Beyerlein, J. Chem. Phys., 78, 7010 (1983).

4. Rutherford, W. M., A Computer Program for Calculating the Transient Behavior of Multicomponent Isotope Separation Cascades, Volume I. Numerical Methods and Description of Program MTRAN, MLM-ML-84-42-0001, Monsanto Research Corporation, Miamisburg, Ohio (February 1984).

5. Rutherford, W. M., A Computer Program for Calculating the Transient Behavior of Multicomponent Isotope Separation Cascades, Volume II. User's Manual for Program MTRAN, MLM-ML-84-42-0002, Monsanto Research Corporation, Miamisburg, Ohio (February 1984).

6. Rutherford, W. M., J. Chem. Phys., 59, 6061 (1973).

7. Mound Activities in Chemical and Physical Research: January-June 1984, MLM-3195, Monsanto Research Corporation, Miamisburg, Ohio (October 1984), p. 18.

8. de la Garza, A., Chem. Engr. Science, 18, 73 (1963).

9. Mound Activities in Chemical and Physical Research: January-June 1981, MLM-2884, Monsanto Research Corporation, Miamisburg, Ohio (December 1981).

10. Mound Activities in Chemical and Physical Research: January-June 19842, MLM-2998, Monsanto Research Corporation, Miamisburg, Ohio (October 1982).

11. Mound Activities in Chemical and Physical Research: January-June 19843, MLM-3125, Monsanto Research Corporation, Miamisburg, Ohio (December 1983), p. 18.

12. Taylor, W. L., J. Chem. Phys., 72, 4980 (1980).

13. Ibbs, T. L., and K. E. Grew, Proc. Phys. Soc. (London), 43, 142 (1931).

14. Puschner, M., Z. Physik, 106, 597 (1937).

15. Atkins, B. E., R. E. Bastick, and T. L. Ibbs, Proc. Roy. Soc. (London), Ser. A 172, 142 (1939).

16. van Itterbeek, A., O. van Paemel, and J. van Lierde, Physica (Utrecht), 13, 231 (1947).

17. Grew, K. E., Proc. Roy. Soc. (London), Ser. A 189, 402 (1947).

18. van Itterbeek, A., and A. de Troyer, Physica (Utrecht), 16, 329 (1950).

19. de Troyer, A., A. van Itterbeek, and G. J. van den Berg, Physica (Utrecht), 16, 669 (1950).

20. Mathur, B. P., and S. C. Saxena, Z. Naturforsch. Teil A., 22, 164 (1967).

21. Grew, K. E., and W. W. Wakeham, J. Phys. B: Atom. Molec. Phys., 11, 2045 (1978).

22. Trengove, R. D., H. L. Robjohns, T. N. Bell, M. L. Martin, and P. J. Dunlop, Physica, 108A, 488 (1981).

23. Mound Activities in Chemical and Physical Research: January-June 1984, MLM-3195, Monsanto Research Corporation, Miamisburg, Ohio (October 1984), p. 14.

24. Taylor, W. L., J. Chem. Phys., 57, 832 (1972).

25. Aziz, R. A., in "Inert Gases, Potentials, Dynamics and Energy Transfer in Doped Crystals," (Springer Series in Chem. Phys., Springer Verlag, New York, 1984), Volume 34, pp. 76-77.

26. Brewer, J., U. S. Air Force Office of Scientific Research, Arlington, VA, No. 67-2793 (1967).

27. Kestin, J., and E. A. Mason, American Institute of Physics Conference Proceedings No. 11, 137 (1973).

28. van Heijningen, R. J. J., J. P. Harpe, and J. J. M. Beenakker, Physica, 38, 1 (1968).

29. Arora, P. S., H. L. Robjohns, and P. J. Dunlop, Physica, 95A, 561 (1979).

30. Trengove, R. D., H. L. Robjohns, T. N. Bell, M. L. Martin, and P. J. Dunlop, Physica, 108A, 488 (1981).

31. Aziz, R. A., W. J. Meath, and A. R. Allnatt, Chem. Phys., 78, 295 (1983).

32. Aziz, R. A., V. P. S. Nain, J. S. Carley, W. L. Taylor, and G. T. McConville, J. Chem. Phys., 70, 4330 (1979).

33. Huemann, K. G., H. Kloppel, and G. Sigl, Z. Naturforsch., 37b, 786 (1982).

34. Gutsykov, V. V., E. S. Lobzhanidze, and M. R. Mirianashvili, Russ J. Phys. Chem., 55(11), 1667 (1981).

35. Jepson, B. E., and G. C. Shockey, Sep. Sci. & Technol., 19(293), 173 (1984).

36. Jepson, B. E., and R. DeWitt, J. Inorg. Nucl. Chem., 38, 1175 (1976).

37. Delphin, W. H., and E. P. Horwitz, Anal. Chem., 50(7), 843 (1978).

38. Schmidhalter, B., and E. Schumacher, Helvetica Chimica Acta, 65(6), 1687 (1982).

Distribution

EXTERNAL

TIC-4500, UC-4 and UC-22 (194)

H. L. Adair, Oak Ridge National Laboratory

J. R. Blair, DOE/Office of Health and Environmental Research

J. Burnett, DOE/Office of Basic Energy Sciences

J. S. Cantrell, Miami University, Oxford, Ohio

G. R. Gartrell, DOE/Dayton Area Office

K. Gschneidner, Iowa University, Ames, Iowa

N. Haberman, DOE/Division of Nuclear Energy

J. N. Maddox, DOE/Office of Health and Environmental Research

J. A. Morley, DOE/Dayton Area Office

L. R. Morss, Argonne National Laboratory

H. A. Schneiderman, Monsanto, St. Louis

F. D. Stevenson, DOE/Office of Basic Energy Sciences

L. Thompson, University of Minnesota

E. L. Venturini, Sandia National Laboratories, Albuquerque

D. White, University of Pennsylvania

Monsanto Reports Library, R2C, St. Louis

INTERNAL

G. C. Abell

W. R. Amos

C. T. Bishop

D. Cain

D. G. Carfagno

V. R. Casella

R. E. Ellefson

W. F. Evans

B. M. Farmer

C. S. Friedman

W. B. Hogeman

C. W. Huntington

B. E. Jepson

B. R. Kokenge

G. T. McConville

D. A. Menke

E. D. Michaels

R. H. Nimitz

W. K. Park

W. M. Rutherford

P. W. Seabaugh

W. E. Sheehan

G. C. Shockey

G. L. Silver

W. L. Taylor

R. J. Tomasoski

R. E. Vallee

C. J. Wiedenheft

W. R. Wilkes

R. W. York

Document Control

Library (15)

Publications

Published by Information Services:
Stephen L. Nowka, Editor